The development of curvature in the porcine radioulna

Jess Pantinople [1] , **Kyle McCabe** [1] , **Keith Henderson** [1] , **Hazel L Richards** [Corresp., 1] , **Nick Milne** [1]

[1] School of Anatomy, Physiology and Human Biology, University of Western Australia, Perth, Western Australia, Australia

Corresponding Author: Hazel L Richards
Email address: hazel.l.richards@gmail.com

Long bone curvature in animal limbs has long been a subject of interest and much work has explored why long bones should be curved. However, the 'when' and 'how' of curvature development is poorly understood. It has been shown that the rat tibia fails to attain its normal curvature if the action of muscles is removed early in life, but it is not clear if this is because the curvature fails to develop or if the bone becomes straighter without the action of muscles. No studies have examined the development of bone curvature in a normally developing quadruped, so this study tracks the course of curvature formation in the radioulna in a series of growing pigs. We also histologically examined the epiphyseal growth plates of these bones to determine if they contribute to the formation of curvature. In all three epiphyseal plates examined, the proliferative zone is thicker and more densely populated with chondrocytes on the cranial (convex) side than the caudal (concave) side. Frost's chondral modelling theory would suggest that the cranial side of the bone is under more compression than the caudal side, and we conclude that this is due to the action of triceps extending the elbow by pulling on the olecranon process. These results support the idea that bone curvature is an adaptation to habitual loading, where longitudinal loads acting on the curved bone cause bending strains that counter the bending resulting from the habitual muscle action.

1   **The development of curvature in the porcine radioulna**

2   Jess Pantinople[1], Kyle McCabe[1], Keith Henderson[1], Hazel L Richards[1], Nick Milne[1]

3   [1]School of Anatomy, Physiology & Human Biology, The University of Western Australia, 35

4   Stirling Highway, Crawley, WA, Australia

5   Corresponding author: Hazel L Richards[1]

6   Email: hazel.l.richards@gmail.com

9   **Abstract**

10   Long bone curvature in animal limbs has long been a subject of interest and much work has

11   explored why long bones should be curved. However, the 'when' and 'how' of curvature

12   development is poorly understood. It has been shown that the rat tibia fails to attain its normal

13   curvature if the action of muscles is removed early in life, but it is not clear if this is because the

14   curvature fails to develop or if the bone becomes straighter without the action of muscles. No

15   studies have examined the development of bone curvature in a normally developing quadruped,

16   so this study tracks the course of curvature formation in the radioulna in a series of growing pigs.

17   We also histologically examined the epiphyseal growth plates of these bones to determine if they

18   contribute to the formation of curvature. In all three epiphyseal plates examined, the proliferative

19   zone is thicker and more densely populated with chondrocytes on the cranial (convex) side than

20   the caudal (concave) side. Frost's chondral modelling theory would suggest that the cranial side

21   of the bone is under more compression than the caudal side, and we conclude that this is due to

22   the action of triceps extending the elbow by pulling on the olecranon process. These results

23   support the idea that bone curvature is an adaptation to habitual loading, where longitudinal

24   loads acting on the curved bone cause bending strains that counter the bending resulting from the

25   habitual muscle action.

26

27

28

29 **Introduction**

30 Long bone curvature in animal limbs has been a subject of interest because it would seem to

31 weaken the bone under weight-bearing conditions – that is, theoretically, curved bones are more

32 prone to failure than straight bones (Bertram and Biewener 1988). Many studies have used strain

33 gauges *in vivo* to examine the strains experienced by curved bones during locomotion (Lanyon

34 and Baggott 1976; Lanyon and Bourn 1979). More contemporary studies have used finite

35 element analysis to model these strains under load (Jade et al. 2014; Milne 2016), while others

36 have studied the relationship between body size and bone curvature (Biewener 1983; Swartz

37 1990; Shackelford and Trinkaus 2002). It is widely understood that altering the mechanical

38 environment of bones affects their growth (Mosley 2000) and metabolism (Uhthoff & Jaworski

39 1979) – for instance, Lanyon (1980) showed that rat tibiae failed to attain normal curvature if

40 loads were removed by sciatic neurectomy and patella tenotomy.

41 In their study, Lanyon (1980) stated that the tibia 'fails to attain' its normal curvature, but did not

42 clarify whether the bone was initially straight and did not develop its normal curvature, or if it

43 was initially curved and became straighter due to the intervention. Searching the literature failed

44 to reveal a clear account of when and how the curvature of such bones appears. Therefore, the

45 first aim of this study is to document when bone curvature develops, using radioulnae from a

46 series of fetal through to six-month-old pigs (*Sus scrofa domesticus*). If the curvature of the

47 radioulnae increases as the young pig grows and begins to use its forelimbs in locomotion, the

48 idea of curvature development as a response to locomotor loading will be supported.

49 The second question addressed here is how such curvature develops. There are two ways a bone

50 may alter its shape or size: endochondral growth during development, and surface remodelling.

51 Frost (1973) described how bones might adjust their shape by surface remodelling in response to

52 loading. Indeed, a curved bone under longitudinal loading would be expected to become

53 straighter, because the concave surface would be under compression - and thus depository - and

54 the convex side would be under tension and thus resorptive. Such a bone would straighten by

55 surface remodelling (drift) under these loads. Conversely, Frost described how an eccentrically

56 loaded bone may become curved by the same mechanism (Frost 1964).

57 Developing bones have epiphyseal growth plates which are the principal means of bone

58 elongation. Frost (1979) described a chondral modelling theory – he suggested that articular or

59   epiphyseal growth cartilages respond to differences in loading: growing faster under

60   physiological compression and slower under tension. Asymmetric growth at the distal femoral

61   epiphysis has been shown to contribute to the orientation of the knee, producing the carrying

62   angle in humans (Tardieu and Trinkaus 1994). Cartilage can also form at the site of repair in

63   bone fractures, and it has been demonstrated, in newborn mice, that these chondrocytes respond

64   in the same way to tension and compression as those concerned with epiphyseal growth (Rot et

65   al. 2014). This is the mechanism by which these bones can straighten during fracture repair (Rot

66   et al. 2014). It is possible that such uneven chondrocyte activity, in response to compressive and

67   tensile loading, may be a way of producing curvature during development.

68   So, our second approach in this study is to examine the cranial and caudal sides of the epiphyseal

69   plates of the porcine radius and ulna, and measure the thickness of the proliferative (growth)

70   zone as well as the density of chondrocytes within this zone. This zone is identifiable as the area

71   where chondrocytes appear flattened and are arranged in columns (Niehoff et al. 2004). If the

72   growing bone is increasing in curvature, it is expected that the proliferative zone on the side of

73   increasing convexity will be larger and more densely packed with chondrocytes than on the

74   concave side.

75

76

Materials & Methods

Twenty-two Duroc boar × Landrace × Large White crossbred pigs which died in the normal course of farming operations were collected from a pig farm in Western Australia (UWA Animal Ethics Committee approval F 69199). The pigs ranged in age from eight days prenatal to 23 weeks postnatal. The ages of the postnatal pigs were obtained from the supplier whereas those of the prenatal pigs were derived by measuring crown-rump length (Ullrey et al 1965). One additional 72-week-old pig was also used to compare the developing pigs with a mature adult. Each pig was weighed, the right radioulna removed and cleaned, and the bone length measured (Table 1). The radioulnae were photographed from the lateral side using a standardised orientation, ensuring the axis of the trochlea notch was vertical in each photograph. From the photographs, 16 landmarks and 80 semilandmarks were digitised in *tpsDig* (Rohlf 2016). The landmarks were chosen to describe the overall shape of the bone, and the semilandmarks were used to characterise the curvature of the bones' caudal and cranial surfaces in the sagittal plane (see Fig 1 and Table 2).

The coordinates of the three sets of semilandmarks, describing the curvature of the posterior ulna and the anterior and posterior radial margins, were translated, scaled and rotated so the proximal semilandmark was at the origin (0,0) and the distal semilandmark had the coordinate (1,0) (after Richmond and Whalen 2001). The largest Y-value among the semilandmarks represented the normalised curvature (i.e. maximum subtense/chord length).

97   Table 1. The age and weight of the pigs and the lengths of the radioulnae used.

98

Age (weeks)	Weight (kg)	length (mm)
-1.14	0.90	50.1
-0.57	1.06	63.4
-0.43	0.95	57.1
0	1.96	67.6
0	1.14	55.4
1	2.18	67.8
2	2.66	69.1
3	3.18	73.8
5	8.10	100.8
6	7.32	103.0
7	11.30	104.3
8	7.92	91.5
9	19.98	121.5
10	25.00	136.2
12	25.00	134.6
13	37.00	149.0
17	57.00	168
20	83.00	198
22	100.00	201
22	100.00	205
22	98.00	185
23	105.00	206
72	180.00	285
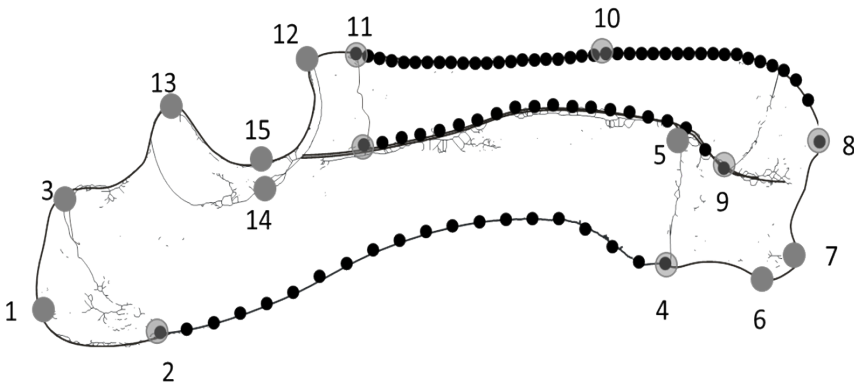
Figure 1. Diagram of a lateral view of the radioulna with the landmarks (numbered grey dots) and semilandmarks (black dots) used: 20 x posterior ulna, 20 x posterior radius and 40 x anterior ulna.

Table 2. The landmarks on the radioulna.

99

100

101

102

103

104

105

106

No.	Definition
1	Apex of olecranon
2	Proximal epiphyseal plate at posterior margin of ulna
3	Proximal epiphyseal plate at anterior margin of ulna
4	Distal epiphyseal plate at posterior margin of ulna
5	Distal epiphyseal plate at anterior margin of ulna
6	Posterior-most point of distal surface of ulna
7	Styloid process of ulna
8	Styloid process of radius
9	Distal epiphyseal plate at posterior margin of radius
10	Middle point of anterior margin of radius
11	Proximal epiphyseal plate at anterior margin of radius
12	Proximal epiphyseal plate at posterior margin of radius (lateral)
13	Midpoint of distal trochlear surface
14	Lateral point of mid-trochlear surface
15	Midpoint of mid-trochlear surface
16	Midpoint of proximal trochlear surface

107   The 96 landmarks were submitted to geometric morphometric analysis in *morphologika*

108   (O'Higgins and Jones 1998). First the landmark sets were Procrustes registered so differences in

109   size, position and orientation among the landmarks were removed and only differences in the

110   shape described by the landmarks remained. The principal components analysis was applied to

111   identify the main patterns of shape variation. As we were interested in the changes in shape that

112   accompany growth, form space was used so that the first principal component (PC1)

113   characterised the shape change with increasing size.

114   Six specimens of different ages (one week prenatal and one, five, nine, 17 and 22 weeks

115   postnatal) were selected and their epiphyseal growth plates examined. The bones were sectioned

116   in the sagittal plane, and samples of the distal ulnar, and proximal and distal radial epiphyseal

117   plates were removed for histological analysis. The proximal ulnar plate was not included

118   because it is a traction epiphysis for the olecranon process and does not form part of the shaft of

119   the ulna (Morgan et al. 2000).

120   Each growth plate sample included the cranial and caudal sides of the epiphysis. The samples

121   were fixed in 10% neutral buffered formalin, rinsed in 0.9% saline and then immersed in rapid

122   decalcifier (Apex Engineering Products Corp., Aurora, IL, USA) for between two and four

123   hours. When the samples were soft enough, they were rinsed in saline and agitated in phosphate-

124   buffered saline (PBS) for 15 minutes, then placed in 30% sucrose solution made in PBS

125   overnight. Samples were then agitated for 15 minutes in a 50:50 solution of PBS and OCT

126   (optimal cutting temperature compound – ProSciTech, Thuringowa, QLD. Australia) before

127   being embedded in OCT, frozen, and sectioned at 40 μm using a cryostat at -20°C (Leica CM

128   3050s). Each block had 25 sections cut and every fifth section was used. The sections were

129   placed on *Superfrost Plus* slides (Lomb Scientific Pty Ltd., Taren Point, NSW, Australia) and air

130   dried overnight. Initially the slides were rinsed and stained in the normal vertical orientation, but

131   this resulted in the loss of some sections (so only four of the six distal radial sections were

132   available). To avoid section loss, subsequent slides were laid horizontally, drops of tap water

133   were used to wash off the OCT, and Gill's Haematoxylin I was applied for one minute before

134   rinsing and mounting with *Kaiser's* aqueous mounting medium.

135   Images of the epiphyseal plates were captured at 100× magnification (Olympus BX50

136   microscope). The images were exported to *tpsDig,* and the thickness of the proliferative zone

137   was measured in five locations 100 μm apart, and the mean recorded (Fig 2).

138   Chondrocytes in the proliferative zone were counted using the optical fractionator probe in

139   S*tereo Investigator* (MBF Bioscience, Williston, VT, USA). This probe is used to directly count

140   proliferating chondrocytes within a defined volume, which then produces an unbiased population

141   estimate without being affected by the size, distribution and orientation of the chondrocytes

142   within this zone (West, Slomianka & Gundersen 1991). The user identifies the region of interest

143   (proliferative zone) in five sections of each tissue block and S*tereo Investigator* randomly selects

144   20 equidistant sampling sites in each section, so 100 sampling sites are counted for each tissue

145   block (Fig 2). From these estimates of chondrocyte population, cell density was estimated by

146   dividing cell count by the total volume of the sampling sites/optical *disectors* (West, Slomianka

147   & Gundersen 1991).

148   Using the statistical package *Genstat* (18th edition, VSN International), Shapiro-Wilks tests were

149   used to confirm normality of data. We then conducted linear regression to determine if the

150   curvatures of the posterior ulna, posterior radius and anterior radius increased significantly with

151   age. Paired t-tests were used to check for differences in the proliferative zone thickness and cell

152   density between the cranial and caudal side of each epiphyseal growth plate.

153

154

155
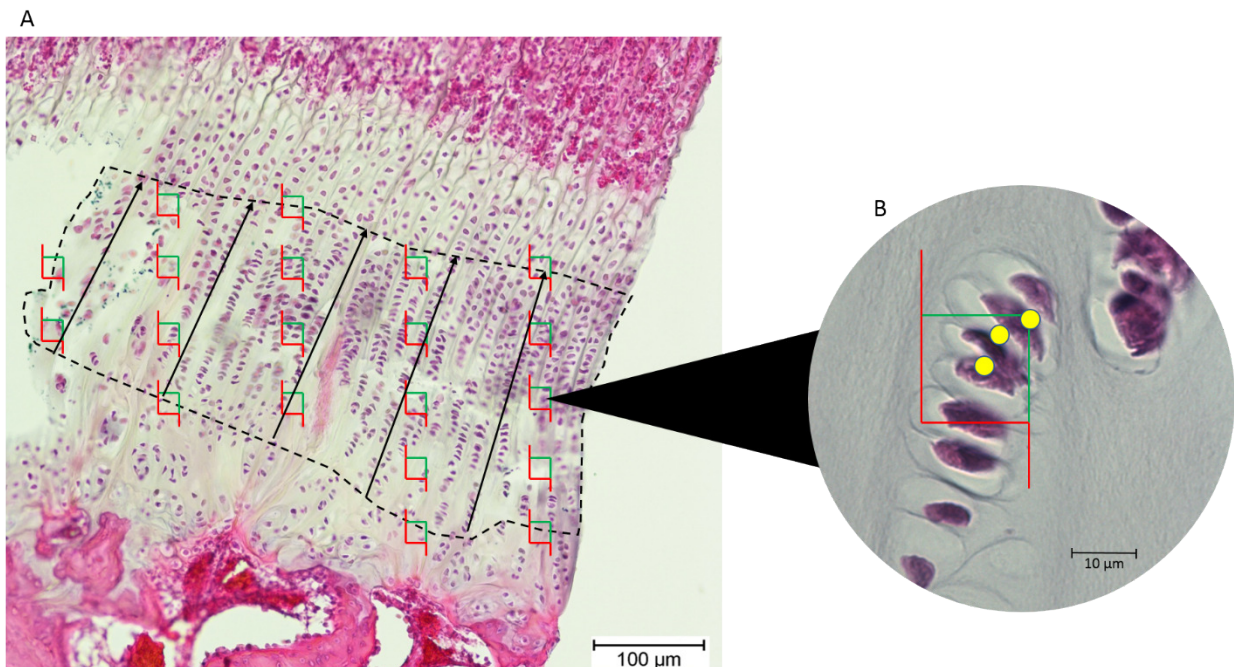
Figure 2. A: An epiphyseal plate with the proliferative zone outlined in dashed lines. Counting frames (green and red boxes) were placed equidistantly across the proliferative zone. The black lines represent the measured thickness of the proliferative zone. B: Inset at higher magnification, showing which cell nuclei (yellow dots) in each counting frame were counted by the software (those wholly within the frame and those intersecting the green boundary).

156

157

158

159

160

161

162

163 **Results**

164 The age, weight and radioulnar length of the 23 pigs is shown in Table 1. These data are all

165 highly correlated with one another (R > 0.95). The 72-week-old pig was excluded from the

166 statistical analyses, but is shown in Fig 3 to compare an adult pig with the developmental series.

167 Figure 3 shows wireframe diagrams representing the extremes of PC1 in a form space analysis of

168 radioulna shape based on the 96 landmarks and semilandmarks. PC1 accounted for 98.5% of the

169 variation and showed a 0.97 correlation with age. This figure shows that the olecranon process

170 becomes larger and the trochlear notch becomes relatively smaller with age. The overall

171 curvature of the radioulna increases and this is particularly evident in the distal areas.

172

173
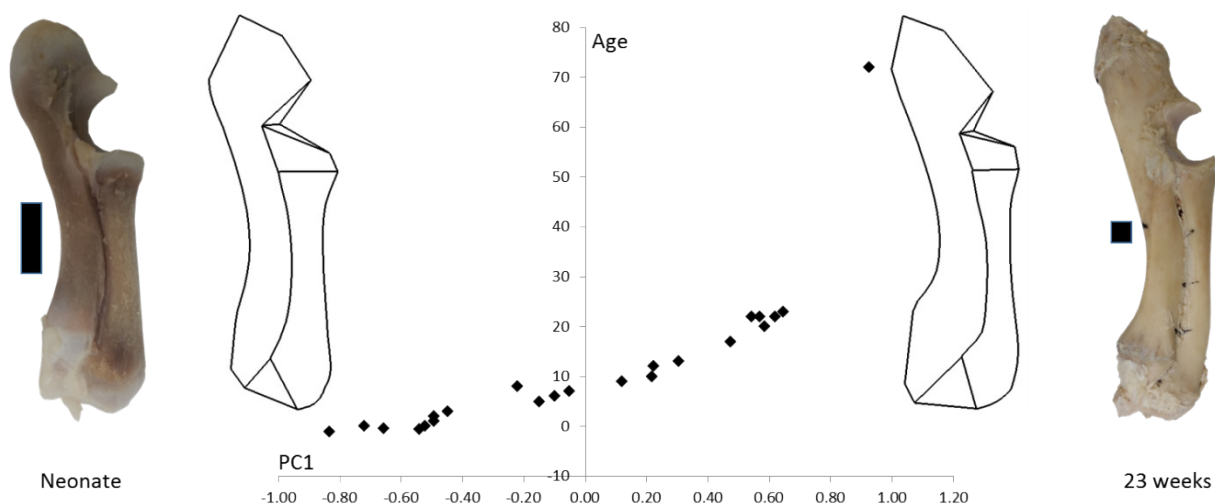
Figure 3. PC1 and age. Form space PC1 (98.5%) is plotted against age. Wireframe diagrams
represent the shapes at the extremes of PC1 (−1 & +1), accompanied by representative
photographs of neonatal and 23-week-old radioulnae (scale bars indicate 1cm).

174

175

176   When the curvature measurements for the posterior ulna and the posterior and anterior margins

177   of the radius are regressed against age, all three curves increase. This increase is only significant

178   for the posterior ulna and anterior radial curves (Fig 4). The curvature value for the 72-week-old

179   pig is also indicated, and shows that the adult curvature is attained in these pigs by 23 weeks of

180   age. Indeed, the anterior radial curve diminishes somewhat in the older pig.

181   The mean thicknesses of the cranial and caudal sides of the epiphyseal proliferative zones are

182   shown in Fig 5. Paired t-tests show that the cranial side is significantly thicker than the caudal

183   side in all three growth cartilages examined ($P < 0.01$). Figure 6 shows the chondrocyte density,

184   and again paired t-tests show these cells are more densely packed on the cranial than the caudal

185   side ($P < 0.01$). Photomicrographs of the cranial and caudal sides of the three cartilage growth

186   plates are shown in fig 7. In each case the cranial side is seen to have a greater chondrocyte

187   density than the caudal side.

188
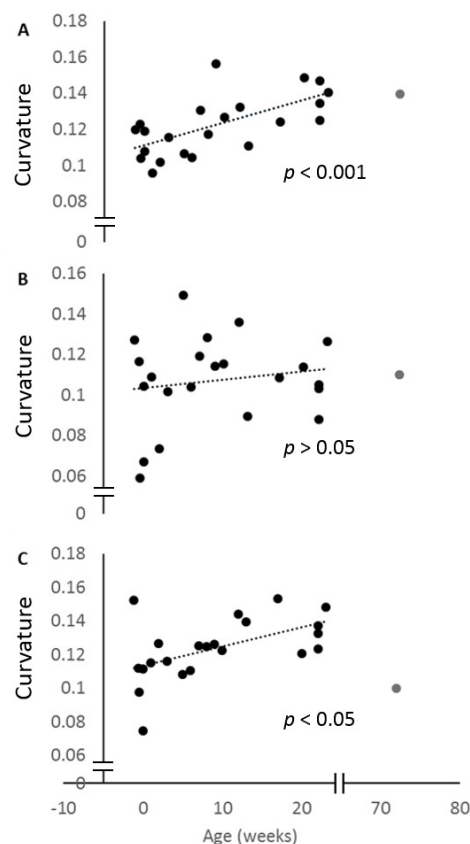
Figure 4. Change in curvature with age. Plots of the normalised curvature versus age for A) posterior ulna, B) posterior radius and C) anterior radius. The values for the 72-week-old pig (grey circle) are included to show how curvatures change beyond 23 weeks, but this specimen was not included in the regression analyses. The p values show the significance of the regression analyses.

189
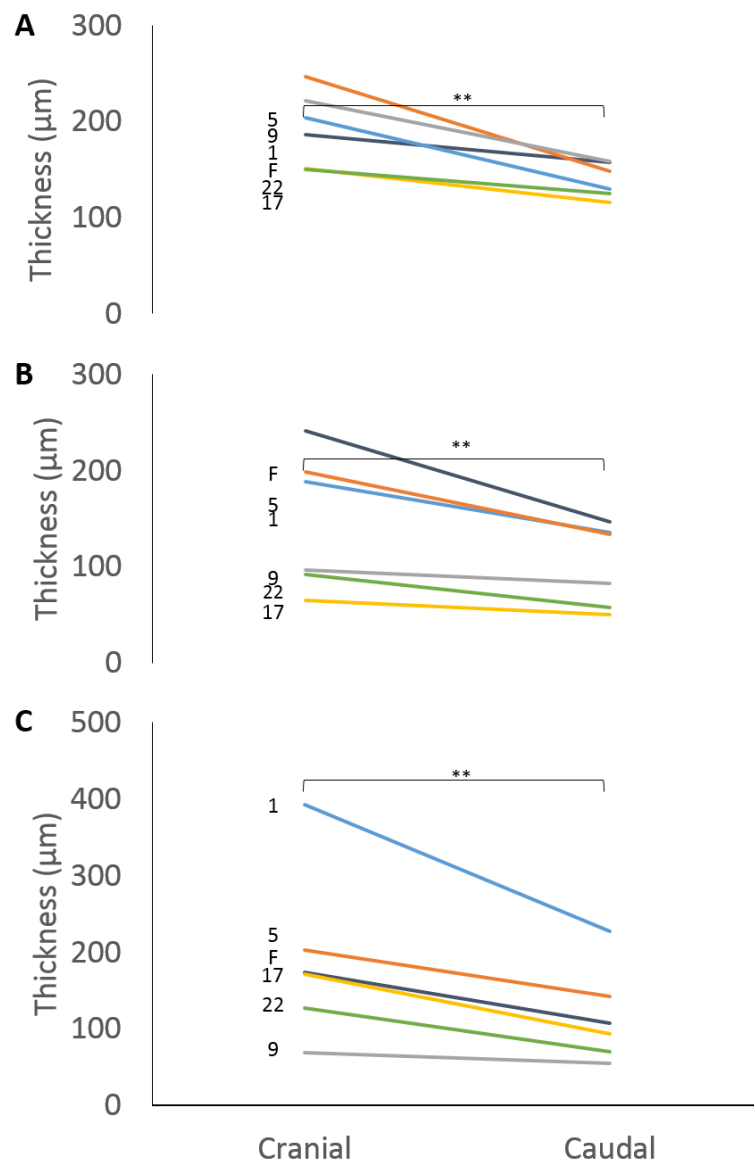
Figure 5. Thickness of the cranial and caudal regions of the proliferative zone in A) distal ulnar, B) proximal radial and C) distal radial epiphyseal growth plates. Individual lines represent a single specimen with age (in weeks) indicated. **Paired t-tests show that that the cranial is significantly thicker than the caudal side ($p < 0.01$).

190
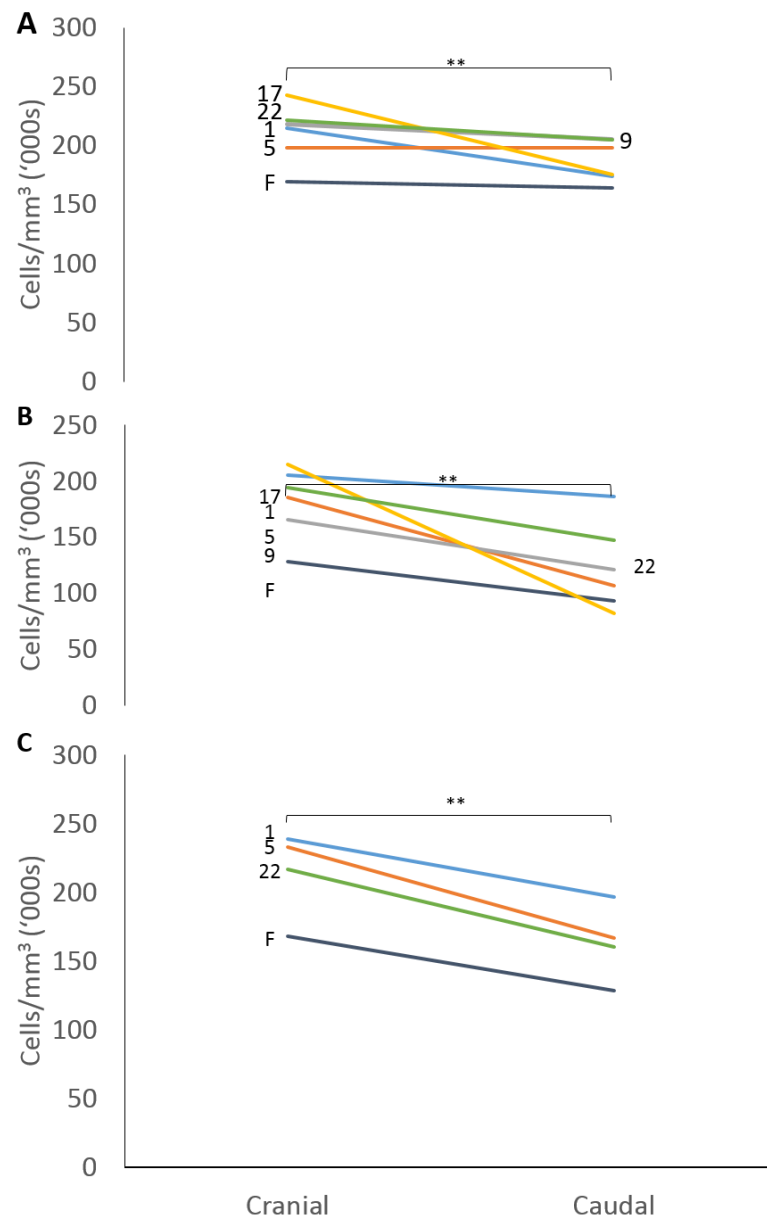
Figure 6. Chondrocyte density in the cranial and caudal regions of the proliferative zone in A) distal ulnar, B) proximal radial and C) distal radial epiphyseal growth plates. Individual lines represent a single specimen with age (in weeks) indicated. **Paired t-tests show that that the cranial has a significantly denser chondrocyte population than the caudal side ($p < 0.01$).

191

192 **Cranial** **Caudal**

193

A B

C D

E F
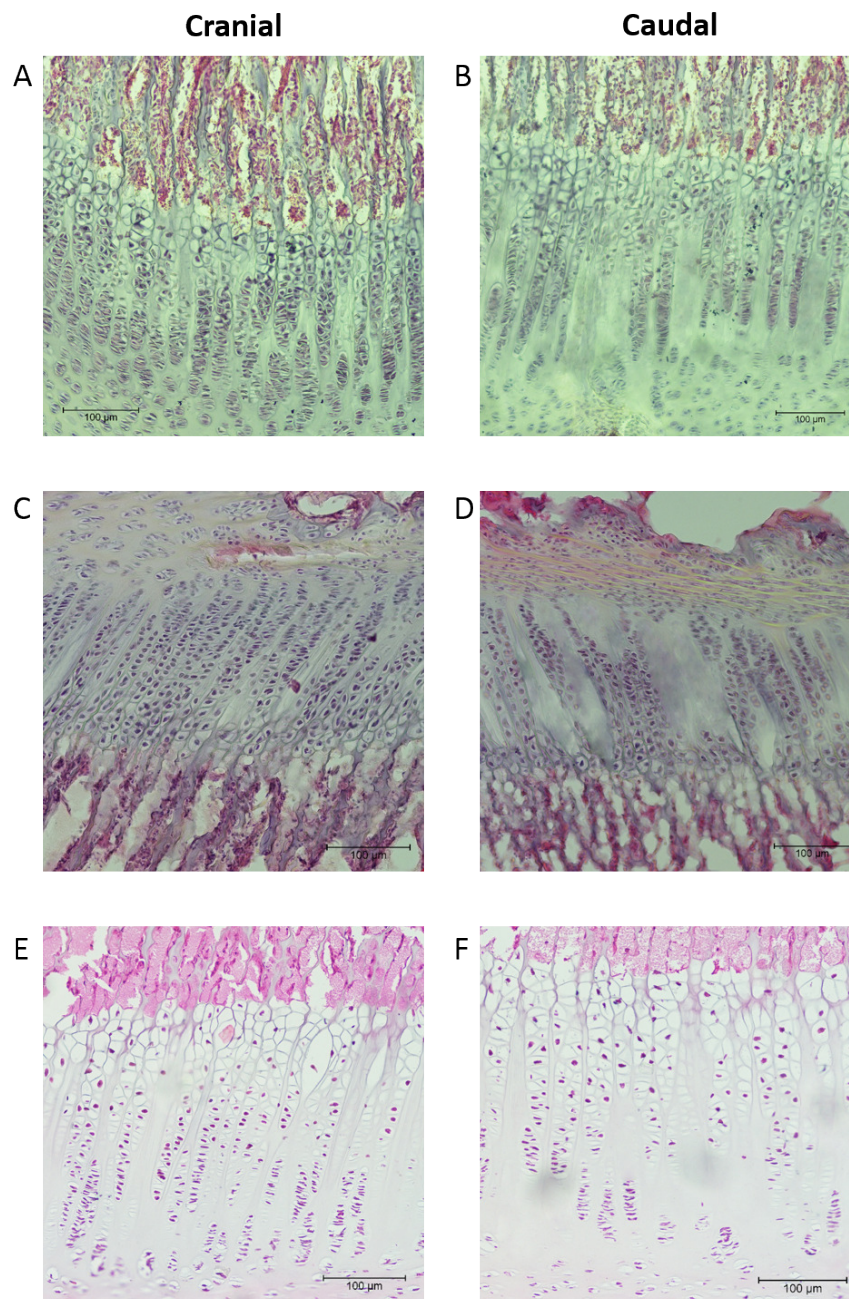
Figure 7. Photomicrographs showing examples of the cranial and caudal growth cartilages from the distal ulna (A and B), proximal radius (C and D) and distal radius (E and F). Sections A to D are 40μm thick and stained with haematoxylin. Sections E and F are 8μm thick and strained with haematoxylin and eosin. All sections are presented at the same magnification (see 100 μm scale bar).

195 **Discussion**

196 This study explored the 'when' and the 'how' of curvature development in the pig radioulna.

197 Both the radius and ulna were found to be caudally curved in near-term fetuses, and this

198 curvature was shown to increase in the first six months of life. Examination of the epiphyseal

199 growth plates showed more chondrocyte activity in the cranial (convex) side than the caudal

200 (concave) side. This establishes a mechanism for the formation and maintenance of bone

201 curvature during development. The differential growth in the cranial and caudal sides of the

202 epiphysis may occur in response to bending strains that place the cranial side in compression and

203 the caudal side in tension (or less compression) (Frost 1964, Milne 2016).

204 The geometric morphometric analyses and regressions of curvature against age showed that

205 radioulnar curvature increased between two weeks prenatal and 23 weeks postnatal. This was

206 true for both the entire bone, as seen in the GM analyses, and for the posterior ulnar and anterior

207 radial margins individually. However, the posterior margin of the radius did not significantly

208 increase in curvature over this period. The slope of the posterior radial curve regression line was

209 shallower, and the variation among curve values greater, than in the other measured curvatures

210 (see Fig 4). It may be that the contact between the posterior ulna and the anterior radius impedes

211 curvature development there, or that clear identification of the anterior surface of the radius was

212 difficult and affected our measurements.

213 Here we examined pigs between two weeks prenatal and 23 weeks postnatal. The prenatal pigs

214 already had some curvature in their radioulnae so it is still uncertain whether this bone is curved

215 throughout fetal life, or is straight during earlier stages of gestation. The initial fetal curvature

216 seen here may be caused by primitive muscle actions *in utero,* causing forelimb movements.

217 Such movements are at their greatest frequency around 15 days before birth (Cohen et al. 2010).

218 Examination of younger fetuses would determine whether the radioulna is indeed curved during

219 early gestation, or if it begins as a straight bone prior to any muscle loading. It is also uncertain

220 whether curvature changes any further beyond 23 weeks, but the 72-week-old specimen suggests

221 that adult curvature is not greater than that of a 23-week-old. The geometric morphometric

222 analysis (Fig 2) and the linear regressions of curvature on age show that the 23-week-old pigs

223 had already attained or even overshot the mature adult curvature.

224 Our analysis of the proliferative zone activity of the epiphyseal growth plates showed that this

225 zone is thicker and more densely populated with chondrocytes on the cranial than the caudal

226 side. In 1979, Frost proposed the chondral modelling theory – within the limits of physiological

227 loading, cartilage grows faster under compression than tension, and grows slower under less

228 compression than more. Numerous studies have supported this theory (e.g. Tardieu and Trinkaus

229 1994; Urban 1994; Hamrick 1999; Congdon et al 2012; Rot et al 2014). Asymmetrical growth of

230 the epiphyseal plates can influence bone shape and was purported to be the mechanism behind

231 both the normal formation of the carrying angle in human femora (Shackelford and Trinkaus

232 2002) and the straightening of bones as fractures heal (Rot et al. 2014). Formation of bone

233 curvature may also be attributable to such asymmetrical epiphyseal plate growth, as our results

234 here suggest.

235 Recently, Henderson and colleagues (2017) showed that the ulnae of terrestrial primates and

236 marsupials are caudally curved, like that of the pig and other terrestrial quadrupeds. Conversely,

237 the ulna of arboreal primates and marsupials is cranially curved. Terrestrial quadrupeds' forearm

238 is dominated by the action of the triceps muscle acting to maintain extension of the elbow, but

239 arboreal species rely on the action of the brachialis muscle to flex the elbow and allow the

240 animal to climb and cling among the branches. The actions of triceps and brachialis place

241 opposite bending strains upon the ulna, and it is proposed that the corresponding opposite

242 curvatures are adaptations to those different bending strains (Milne 2016). If bone and cartilage

243 are stimulated to grow by compressive loading and growth is inhibited by tension (Frost 1979),

244 then this would provide a mechanism by which these opposite curvatures develop in terrestrial

245 and arboreal species. In the case of the developing pig, where triceps acts to maintain stance

246 during locomotion*, the radioulna would experience cranial bending (with more compression on

247 the cranial side). These bending strains may be responsible for the greater proliferation of

248 cartilage cells in the cranial than the caudal side of the growth plates, and thus may be

249 responsible for the development of the caudal curvature (caudal concavity) observed here.

250

251 **Conclusions**

252 Until recently, the timing and the mechanism of bone curvature formation was unknown. Lanyon

253 (1980) saw a straightening of the rat tibia in the absence of muscle action but did not specify

254   whether the bone curvature decreased or failed to form in the first place. The present study is the

255   first to document that curvature does exist early in life, and increases as the animal grows.

256   Frost's (1979) chondral modelling theory was used to explain how congruent joint surfaces are

257   maintained and how the femoral carrying angle forms – however, until now this mechanism has

258   not been explicitly associated with curvature formation. The results presented here suggest that

259   chondral modelling is also applicable to the formation of bone curvature. Further, it seems likely

260   that the formation of radioulnar curvature may be a direct result of the habitual action of the

261   triceps muscle, inducing a strain gradient that drives chondral modelling in the epiphyseal

262   growth plates of the growing bone. This was a pilot study exploring the development of

263   curvature and a possible mechanism of curvature formation; it is hoped that future studies will

264   test these ideas and further explore the mechanism of long bone curvature formation.

265

266   **Acknowledgements**

267   John Kopriwa provided the specimens used in the study. Lutz Slomianka, Mary Lee and Guy

268   Ben-Ary assisted in the preparation and analysis of the cartilage samples.

269

References

Biewener, AA 1983, 'Allometry of quadrupedal locomotion: the scaling of duty factor, bone curvature and limb orientation to body size', *Journal of Experimental Biology*, vol. 105, pp. 147-171.

Cohen, S, Mulder, EJH, van Oord, HA, Jonker, FH, Parvizi, N, van der Weijden, GC & Taverne, MAM 2010, 'Fetal movements during late gestation in the pig: A longitudinal ultrasonographic study', *Theriogenology*, vol. 74, no. 1, pp. 24-30.

Congdon, KA, Hammond, AS & Ravosa, MJ 2012, 'Differential limb loading in miniature pigs (Sus scrofa domesticus): a test of chondral modeling theory', *The Journal of Experimental Biology*, vol. 215, no. 9, pp. 1472-1483. Available from: PMC.

Frost, HM 1964, *The Laws of Bone Structure*, Charles C Thomas, Springfield, IL.

Frost, HM 1973, *Bone modelling and skeletal modelling errors*, Charles C. Thomas, Springfield, IL.

Frost, H 1979, 'A chondral modeling theory', *Calcified Tissue International*, vol. 28, no. 1, pp. 181-200.

Hamrick, MW 1999, 'A Chondral Modeling Theory Revisited', *Journal of Theoretical Biology*, vol. 201, no. 3, pp. 201-208.

Henderson, K, Pantinople, J, McCabe, K, Richards, H & Milne, N 2017 'Forelimb bone curvature in terrestrial; and arboreal mammals', *PeerJ*, 5, p:e3229

Jade, S, Tamvada, KH, Strait, DS & Grosse, IR 2014, 'Finite element analysis of a femur to deconstruct the paradox of bone curvature', *Journal of Theoretical Biology*, vol. 341, pp. 53-63.

Lanyon, LE & Baggott, DG 1976, 'Mechanical function as an influence on the structure and form of bone', *The Journal of bone and joint surgery. British volume*, vol. 58-B, no. 4, p. 436-443.

Lanyon, LE & Bourn, S 1979, 'The influence of mechanical function on the development of remodeling of the tibia' *The Journal of bone and joint surgery. British volume*, vol. 61-A pp263-272.

Lanyon, LE 1980, 'The influence of function on the development of bone curvature. An experimental study on the rat tibia', *Journal of Zoology*, vol. 192, no. 4, pp. 457-466.

300   Milne, N 2016, 'Curved bones: An adaptation to habitual loading', *Journal of Theoretical*

301   *Biology*, vol. 407, pp. 18-24.

302   Morgan, JP, Wind, AP & Davidson, AP 2000, *Hereditary bone and joint diseases in the dog:*

303   *osteochondroses, hip dysplasia, elbow dysplasia*, Schlütersche, Hanover.

304   Mosley, JR 2000, 'Osteoporosis and bone functional adaptation: Mechanobiological regulation of

305   bone architecture in growing and adult bone, a review', *Journal of Rehabilitation*

306   *Research and Development*, vol. 37, no. 2, pp. 189-99. Available from: ProQuest Central.

307   Niehoff, A, Kersting, UG, Zaucke, F, Morlock, MM & Brüggemann, G-P 2004, 'Adaptation of

308   mechanical, morphological, and biochemical properties of the rat growth plate to dose-

309   dependent voluntary exercise', *Bone*, vol. 35, no. 4, pp. 899-908.

310   O'Higgins, P & Jones, N 1998, 'Facial growth in Cercocebus torquatus: an application of three-

311   dimensional geometric morphometric techniques to the study of morphological variation',

312   *Journal of Anatomy*, vol. 193, no. Pt 2, pp. 251-272. Available from: PMC.

313   Richmond, BG & Whalen, M 2001, 'Forelimb function, bone curvature and phylogeny of

314   *Sivapithecus*', in *Phylogeny for the Neogene hominoid primates of Eurasia*, eds P

315   Andrews, L de Bonis & GD Koufos, Cambridge University Press, Cambridge, pp. 326-

316   348.

317   Rohlf, FJ 2004, *tpsDig*, Stony Brook Morphometrics. Available from:

318   http://life.bio.sunysb.edu/morph/.

319   Rot, C, Stern, T, Blecher, R, Friesem, B & Zelzer, E 2014, 'A Mechanical Jack-like Mechanism

320   Drives Spontaneous Fracture Healing in Neonatal Mice', *Developmental Cell*, vol. 31, no.

321   2, pp. 159-170. [2016/02/29].

322   Shackelford, LL & Trinkaus, E 2002, 'Late Pleistocene human femoral diaphyseal curvature',

323   *American Journal of Physical Anthropology*, vol. 118, no. 4, pp. 359-370.

324   Swartz, SM 1990, 'Curvature of the forelimb bones of anthropoid primates: Overall allometric

325   patterns and specializations in suspensory species', *American Journal of Physical*

326   *Anthropology*, vol. 83, no. 4, pp. 477-498.

327   Tardieu, C & Trinkaus, E 1994, 'Early ontogeny of the human femoral bicondylar angle',

328   *American Journal of Physical Anthropology*, vol. 95, no. 2, pp. 183-195.

329   Uhthoff, H & Jaworski, Z 1978, 'Bone loss in response to long-term immobilisation', *Bone &*

330   *Joint Journal*, vol. 60-B, no. 3, pp. 420-429.

331   Ullrey, DE, Sprague, JI, Becker, DE and Miller, ER, 1965, 'Growth of the swine fetus', *Journal*

332   *of Animal Science*, vol. 24, no. 3, pp.711-717.

333   Urban, JPG 1994, 'The chondrocyte: a cell under pressure', *Rheumatology*, vol. 33, no. 10, pp.

334   901-908.

335   West, MJ, Slomianka, L & Gundersen, HJG 1991, 'Unbiased stereological estimation of the total

336   number of neurons in the subdivisions of the rat hippocampus using the optical

337   fractionator', *The Anatomical Record*, vol. 231, no. 4, pp. 482-497.

338